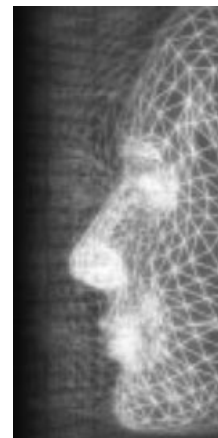


Virtual Humans and Social Agents

# Modeling and simulating the deformation of human skeletal muscle based on anatomy and physiology

By Robson R. Lemos\*, Jon Rokne, Gladimir V. G. Baranoski, Yasuo Kawakami and Toshiyuki Kurihara



*This paper describes the modeling and simulation of the deformation of human skeletal muscle at different structural levels based on sound scientific principles, experimental evidence, and state-of-art muscle anatomy and physiology. The equations of a continuum model of a muscle with realistic architecture, including internal arrangement of muscle fibers and passive structures, and deformation, including activation relations, was developed and solved with the finite element method. The continuum model is used as the basis of a strategy for controlling muscle deformation using activation relations. In order to demonstrate the functionality of the model, it was used to investigate force production and structural changes during contraction of the human tibialis anterior for maximally and submaximally activated muscle behavior. From a comparison with experimental data obtained from ultrasound imaging, we concluded that the modeling and simulation of the continuum based on physiologically meaningful parameters as described in the paper is both an excellent predictor of force production observations and of changes in internal geometry under various test conditions. It is therefore a valuable tool for controlling muscle deformation during movement. Copyright © 2005 John Wiley & Sons, Ltd.*

KEY WORDS: physically-based muscle modeling; medical three-dimensional simulation

## Introduction

Two major constituents of mammals are the skeleton and the skeletal muscles. In most mammals the skeletal muscle accounts for at least 40% of whole body mass;<sup>1</sup> thus, it is an important feature. Additionally, whereas the skeleton is a rigid framework, the skeletal muscles deform in response to contractions of muscle fibers. These deformations are visible when mammals move. In computer animation of virtual mammals, in particular, humans, the deformations of muscles therefore have to be taken into account. However, the models currently

available typically do not allow for muscle deformation. This means that the increasing demand for realism and predictability in computer graphics<sup>2</sup> and bioengineering applications<sup>3</sup> cannot be met. The model described in this paper is a step towards the automatic modeling of the deformation in virtual humans in a predictive manner through the interrelationships of the muscle anatomy and function with applications in computer graphics. Similarly, the model can simulate a complex muscle structure so that muscle function can be investigated in bioengineering.

A three-dimensional structural continuum model of whole muscle was developed.<sup>4</sup> The model was applied to simulate contraction and the associated deformations of a skeletal animal muscle for maximally activated muscle behavior.<sup>5</sup> The model was used to investigate force production and structural changes during contraction of the human tibialis anterior (TA) for maximally and submaximally activated muscle behavior using

\*Correspondence to: Robson R. Lemos, Universidade de Caxias do Sul, Department of Computer Science, Rua Francisco Getulio Vargas, 1130, 95070-560 Caxias do Sul, RS, Brazil.  
E-mail: rlemos@ucs.br

Contract/grant sponsors: CAPES-Brazil, Universidade de Caxias do Sul (Brazil); University of Calgary (Canada).

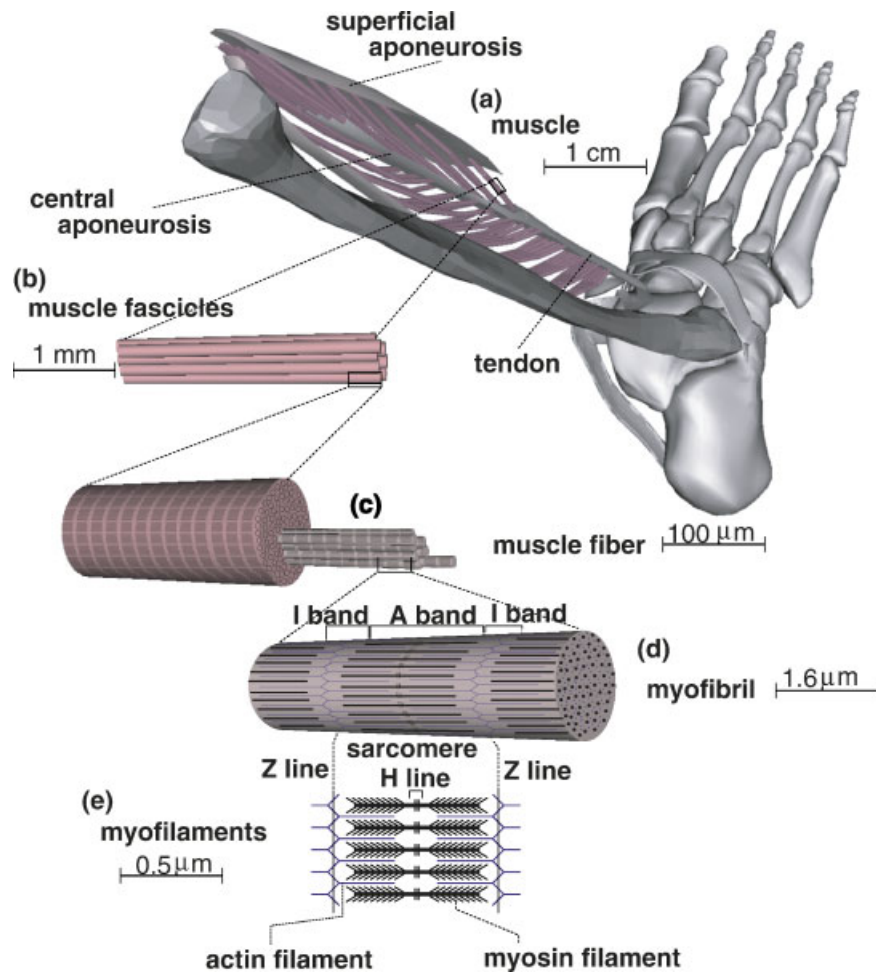


Figure 1. Structural levels. (a) muscle (fiber-aponeurosis-tendon complex); (b) fiber bundle or fascicle; (c) fiber (cell); (d) myofibril; (e) sarcomere (contractile unit).

activation relations based on physiologically meaningful parameters. The novel feature of the approach is that it incorporates several structural levels of representation to predict force relationship, taking into account activation relations for controlling muscle deformation, starting from the muscle fiber level (Figure 1).

The aim of this study is, therefore, to present the modeling and simulation of the deformation of human skeletal muscles at different structural levels for maximally and submaximally activated muscle behavior. In the next section, relevant literature is presented and biological considerations regarding muscle modeling are provided. In the third section continuum model of muscle, the three-dimensional continuum model of muscle is presented. In the fourth section modeling the human Tibialis Anterior muscle, the modeling of the human TA muscle is described. In the fifth section,

muscle deformation simulation and evaluation are shown. Finally, a discussion and some conclusions are presented in the eighth and ninth sections, respectively.

## Related Work and Biological Considerations

Computer graphics researchers have proposed models in which individual muscles are represented in an anatomically appropriate manner.<sup>6,7</sup> In the models proposed by Chen and Zeltzer<sup>8</sup> and Ng-Thow-Hing and Fiume,<sup>9</sup> muscle deformation is obtained based on mechanical principles. Non-linear properties of muscles were neglected, however.

The principal elements of the muscle structure, which form the skeletal muscle architecture, are known as the fiber-aponeurosis-tendon complex (Figure 1), a highly non-linear constrained system. In computer graphics, previous work by Teran *et al.*<sup>10</sup> included non-linear properties of muscle. The muscle geometry was extracted from the segmented visible human dataset.<sup>11</sup> This dataset does not contain detailed information about the fiber-aponeurosis-tendon complex. Simplifying assumptions for the aponeurosis properties and structure (a thin layer of connective tissue within a muscle to which fiber attach) were therefore made in the modeling of the muscle behavior (and its corresponding anatomy). The aponeurosis plays an important role in the internal and external muscle deformation.<sup>12</sup> According to Reference [10] the tendon/aponeurosis and fiber information could be improved with the aid of scanning technologies or anatomy experts. In biomechanics, Gielen *et al.*<sup>13</sup> described a planar model representing the mid-sagittal plane of the muscle belly. Oomens *et al.*<sup>14</sup> extended the mid-sagittal plane continuum model of Gielen *et al.*<sup>13</sup> to a model with a more realistic three-dimensional geometry. According to these authors,<sup>14</sup> further improvements of the model are needed in the transverse plane geometry in order to obtain the actual three-dimensional representation of the muscle. Fernandez *et al.*<sup>15</sup> presented an anatomically based finite element geometric model to match human specific musculo-skeletal system. Blemker *et al.*<sup>16</sup> used a non-linear finite element analysis to simulate a three-dimensional skeletal muscle, simplified by axial symmetry. In cardiac and skeletal muscles models, it has been pointed out that the orientation of muscle fibers and activation, has a large influence on stresses and strains.<sup>3</sup> Because of this, a model of skeletal muscle should have a detailed description of the three-dimensional architecture and deformations so as to have predictive value. The model should also include a mechanism to automatically produce muscle deformation during movement.

Based on spatial distribution analysis<sup>17</sup> it has been shown that some muscles are compartmentalized. Assuming that parts of the muscle corresponding to neuromuscular compartments are activated separately during contraction as a result of some type of different functional or task-specific roles during movement, an interesting force production related property can be investigated. This force production related property, which is difficult to determine in human muscles, is known as the non-linear summation of force<sup>18</sup> in which *submaximally activated muscle behavior* during contractions can be investigated. Studies in animal muscles<sup>18</sup>

indicate that the non-linear summation of force has functional implications for controlling skeletal muscle during movement.

## Continuum Model of Muscle

A non-linear dynamic finite element model (FEM) that allows for designing and simulating a general, variable muscle fiber architecture was developed. A full explanation of the continuum model can be found in Reference [4]. For completeness the general features of the model are also included here.

One possible way to formulate the non-linear equations of motion is by means of the principle of virtual work (PVW). The PVW states that the equations of motion of a deformable body are equivalent to the satisfaction of the following simple scalar equation:

$$IVW - EVW \equiv 0 \quad (1)$$

identically for all virtual displacement fields. In the equation above, IVW is the total internal virtual work and EVW is the total external virtual work performed during the deformation of the body. The PVW can be modified to take into account geometric constraints by the addition of new variables ('Lagrange multipliers').

One of the advantages of the formulation in terms of the PVW is that it is amenable to direct numerical implementation. The system of non-linear equations derived from the PVW were solved using the full Newton's method and the secant method<sup>19</sup> so that execution speeds and accuracies of solutions could be compared. In order to include time-dependent effects, such as viscosity and inertia, the Houbolt implicit time integration technique<sup>20</sup> was adopted.

As the tissue matrix deforms, it performs external and internal virtual work. The applied external forces, as well as the forces of inertia, will perform a small amount of work on the virtual displacements. This work is the external virtual work (EVW). As an example, if concentrated forces  $\mathbf{f}$  are applied at given points of the body, the external virtual work can be obtained as:

$$EVW = \sum \mathbf{f} \cdot \delta \mathbf{u} - \int_V \rho \ddot{\mathbf{u}} \cdot \delta \mathbf{u} dV \quad (2)$$

Here, the summation extends over the number of external forces. A dot represents the ordinary inner ('dot') product of vectors. The mass density in the reference configuration is denoted by  $\rho$ , the reference volume by  $V$ , and the acceleration vector by  $\ddot{\mathbf{u}}$ .

At the same time, a deformable body will sustain an IVW representing the work done by the internal distributed forces (stresses) on the small changes of deformation. The formulation for the IVW for passive and active muscle soft tissues is described below. Moreover, for the active muscle fibers a strategy for controlling muscle deformation using activation relations is described.

### Passive Soft Tissue Modeling

In the large deformation regime, we first need to describe the kinematics of the deformation. For that, we use the deformation gradient tensor  $\mathbf{F}$  which is a mapping from the undeformed reference configuration to the deformed spatial configuration.<sup>2</sup> From the deformation gradient we can extract all the information needed about the state of strain by eliminating the rotational component. One way to do this is by calculating the right Cauchy–Green tensor<sup>2</sup> as  $\mathbf{C} = \mathbf{F}^T \mathbf{F}$ .

A material whose constitutive behavior is characterized by specifying its internal energy stored per unit volume is called a hyperelastic material. We can define specific functional forms of its internal energy. Using the functional form known as the Mooney–Rivlin relation<sup>2</sup> the first Piola–Kirchhoff stress tensor, a convenient measure of stress, can be obtained as:

$$\mathbf{T} = 2a\mathbf{F} + 2b(\mathbf{F}\text{tr}(\mathbf{C}) - \mathbf{F}\mathbf{C}) - p\mathbf{I} \quad (3)$$

where  $a$  and  $b$  are material parameters which obey the scalar equation,  $a + b = \frac{1}{2}\mu$ ,  $\mu$  is a material parameter known as ground-state shear modulus,<sup>2</sup> and  $p$  is a Lagrange multiplier representing a hydrostatic pressure associated with the incompressibility constraint.

In this context, the internal virtual work within a referential volume  $v$  is the work of the internal forces, or stresses, and is given by:

$$\text{IVW}_{\text{tissue}} = \int_V \text{tr}(\mathbf{T}^T \delta \mathbf{F}) dV \quad (4)$$

where  $\text{tr}$  represents the trace of a tensor.

In order to represent the wrinkling observed in tendons, a constitutive passive equation with pseudo-wrinkling of the fibrous tissue of the tendon is included. The pseudo-wrinkling of the fibrous tissue is assumed to obey an exponential constitutive law

$$Nt = \sigma t \cdot At \quad (5)$$

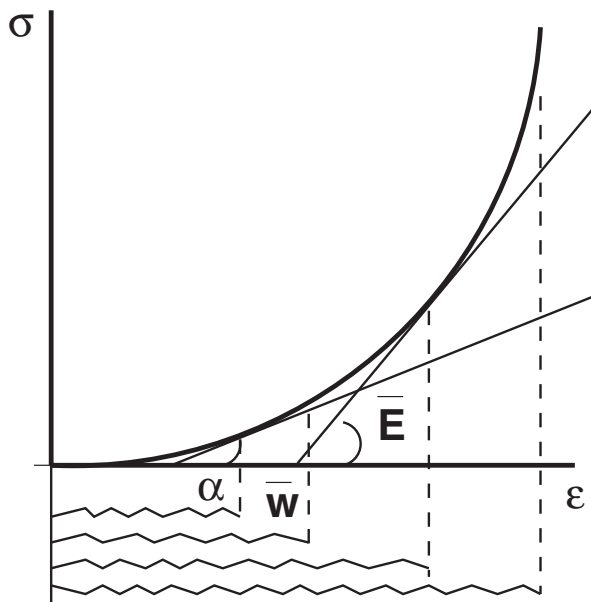


Figure 2. Tendon fibrous tissue behavior.

where  $At$  is the cross-sectional area of the tendon and  $\sigma t$  is the stress ( $\text{N}/\text{mm}^2$ ) given by the following equation

$$\sigma t = \begin{cases} \bar{E} \left[ \epsilon - \bar{w} \left( 1 - e^{-\left(\frac{1-\alpha}{\bar{w}}\right)\epsilon} \right) \right] & \text{for } \epsilon \geq 0 \\ \alpha \bar{E} \epsilon & \text{for } \epsilon < 0 \end{cases} \quad (6)$$

$\alpha$  and  $\bar{w}$  are parameters to control the toe region of the constitutive equation and  $\epsilon$  is the strain, that is, the elongation of the tendon member divided by the length of the original force-free configuration (Figure 2).

The internal virtual work of the tendon is given by

$$\text{IVW}_{\text{tendon}} = Nt \delta e \quad (7)$$

where  $\delta e$  is the small variation in the elongation produced by the virtual displacements of the endpoints of the tendon element.

### Active Soft Tissue Modeling

In order to represent the active soft tissues, the active elements are distributed unidirectionally within the muscle tissue. The force–length relation in fully activated isolated fibers or fiber bundles is well known (Figure 3). Each point on the graph representing the force–length relation of a muscle fiber is obtained by means of a separate experiment, whereby the muscle is first passively brought to a desired length, and only then activated to the maximum at constant length (namely,

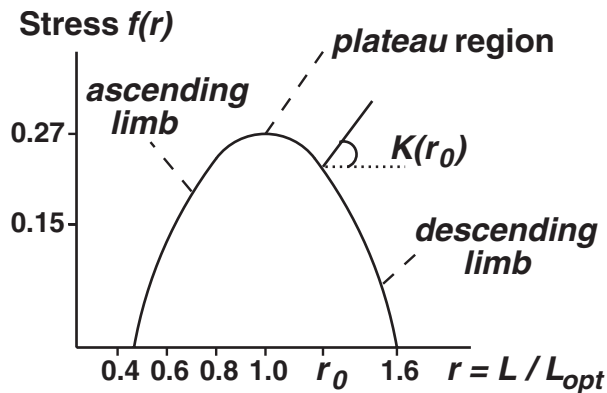


Figure 3. Muscle fiber behavior.

under isometric conditions). Studies have shown that, after arriving at a point in the force-length relation, if the length of the muscle is further increased or decreased without reducing the activation, the force will not follow the graph of the basic force-length relation. Instead, it will tend to follow approximately a straight line with a positive slope.<sup>21</sup> Otherwise, the behavior would be unstable whenever the starting point lies in the descending limb of the force-length relation. In the present model, the ability of specifying the value of that positive stiffness associated with extra lengthening at full activation is included in the force-length relation.

In this context, the force-length relation is represented by the parabola:<sup>22</sup>

$$f(r) = -0.772r^2 + 1.544r - 0.494 \quad (8)$$

expressing the normal stress (N/mm<sup>2</sup>) as a function of the ratio  $r = L/L_{opt}$  between current fiber length,  $L$ , and optimal fiber length,  $L_{opt}$ . The optimal length corresponds to the vertex of the parabola. We assume, somewhat arbitrarily, that the stress corresponds to the presence of 10 000 individual fibers per mm<sup>2</sup>. The number of fibers  $n_f$  running through a given element can be specified, so that the total force for the active fibers within that element is given (in Newtons) by:

$$F_{act} = a [f(r_0) + k(r_0)(r - r_0)] \frac{n_f}{10\,000} \quad (9)$$

where  $a$  is an activation parameter ( $0 \leq a \leq 1$ ), and  $r_0$  is the value of  $r$  upon first activation. The positive stiffness  $K(r_0)$  represents the behavior for active elongations beyond the initial length. In other words, the enforcement of stability through positive stiffness introduces a memory effect at the fiber level. The muscle fiber remembers the current length when it was first activated

until the activation disappears. When the activation disappears, the current length is forgotten and a new current length will take place upon the reappearance of any level of activation. This activation relation is amenable to direct implementation of a strategy for controlling muscle deformation during movement.

The contribution to the IVW of a given active element when the velocity dependence is neglected is given by:

$$IVW_{fiber} = \sum F_{act} \delta e \quad (10)$$

where  $\delta e$  is the small variation in the elongation produced by the virtual displacements of the endpoints of the active element.

The contribution for the IVW of a given active element when the FEM is time-dependent is given by:

$$IVW_{fiber} = \sum f(v) F_{act} \delta e \quad (11)$$

where  $f(v) = 1 - \tanh(v/v_0)$  is the force-velocity dependence,  $v$  is speed in mm/second, and  $v_0$  is the maximal velocity of shortening of a given muscle. It corresponds to a multiplicative factor into the constitutive law (Equation 9) due to the inclusion of a viscous component in the muscle fibers.

### Strategy for Controlling Muscle Deformation Using Activation Relations

In the continuum model a simple strategy for controlling muscle deformation and muscle force using activation relations is introduced. For that the following quantities have to be defined: the attachment sites of the muscle within the skeletal system; the kinematics of skeletal system for a given target movement; the amount of activation of each muscle during the target movement; and, the spatial location of anatomical compartments in the muscle, if applicable.

The muscle-tendon length (and muscle fiber length) in the passive state can be obtained from the attachment sites of the muscle within the skeletal system. The speed that the muscle-tendon length was shortened or stretched during movement can be obtained from the kinematics of the skeletal system. In the continuum muscle model the muscle force and muscle deformation will be obtained as a function of muscle-tendon length, the contractile speed of the muscle-tendon length, and amount of activation.

In the model we assume that all muscle fibers are recruited at the same time (i.e., uniformly) to reach a given amount of activation. A possible choice of

non-uniform recruitment of muscle fibers would be to consider the fiber type distribution of a given muscle and recruit groups of muscle fibers (motor units) non-uniformly according to some type of principle (e.g., some motor units recruited first and other motor units recruited progressively). However, the force control mechanism in skeletal muscle is also influenced by other factors and a comprehensive force control paradigm is not yet available.

In the proposed activation–recruitment relation, the muscle fiber non-uniformities are included in the muscle structure. The initial internal muscle structure for each hexahedra element (Figure 7) in the passive state is used to calculate the initial ratio of fiber length  $r$  and optimal fiber length  $L_{opt}$  for each fiber (Equation 9). This ratio turns out to be non-uniform, and it is used to predict muscle force over the entire range of motion. Therefore, in the activation relation all the muscle fibers will be recruited at the same time but each muscle fiber will be at a different position in the force–length relationship (Figure 3).

In the case of compartmentalized muscles which contain anatomical compartments each having a separate innervation branch we adopt the activation relation in separate parts of the muscle. This control strategy might be used for a group of individual muscles. In this way submaximally activated muscle behavior during contraction of compartmentalized muscles can be investigated as well as the implications in muscle deformation and force production.

## Modeling the Human Tibialis Anterior Muscle

A current trend in computer graphics is to compare theoretical results (results provided by the model) with experimental results (in our case, results obtained by ultrasound medical imaging assessment) so that their accuracy can be directly examined and the models can be used in a predictive manner. This section details various aspects of our method.

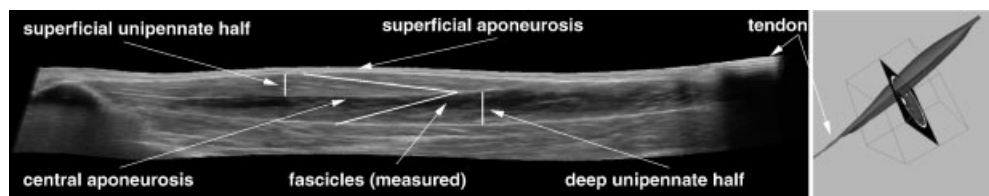


Figure 4. Longitudinal ultrasound image and polygonal boundary of the human TA.

## Experimental Muscle Deformation Measurement

A detailed description of the experimental protocol and muscle deformation measurement performed for the model can be found elsewhere.<sup>23</sup>

In order to investigate structural changes and force production in the human TA during contraction, relaxed and activated fascicle lengths (or fiber bundles), angle of pennation (i.e., angle between the muscle's line-of-action and the direction of the muscle fibers), and external forces were measured.

For the fascicle lengths and angles of pennation measurement, longitudinal sectional images of the human TA were obtained using a real-time ultrasound apparatus. For passive deformations, measurements of the muscle deformation geometry were taken at ankle angles of  $-10^\circ$  (dorsiflexion direction),  $0^\circ$  (the foot at right angle to the shank),  $+10^\circ$ ,  $+20^\circ$ , and  $+30^\circ$  (plantarflexion direction) (Figure 5). Isometric contractions (muscle at constant length) during maximum voluntary contraction (MVC) were obtained, as well. For isometric contractions, during different force levels (20%, 40%, 60%, 80%, and 100% MVC), measurements of the muscle deformation geometry were taken at the ankle angle of  $+30^\circ$ .

The tendon force was estimated 281.42 N at an ankle angle of  $+30^\circ$  during MVC using a similar technique described in Ito *et al.*<sup>23</sup>

## External and Internal Muscle Geometry Reconstruction

The external geometry was found from cross-sectional images obtained by magnetic resonance imaging. The actual internal geometry was found from longitudinal images obtained by ultrasonography. The hexahedral mesh was obtained from polygonal boundaries for TA (Figure 4) using the software *Truegrid*. The position and orientation the fascicle for the measurements were approximated in the internal geometry.

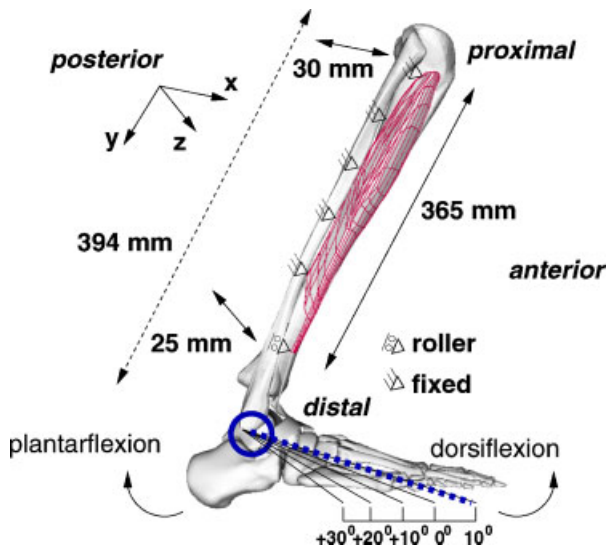


Figure 5. Human TA hexahedral mesh.

The resultant hexahedral mesh had 390 elements (i.e., eight-node brick-like element) including elements for muscle tissue, aponeurosis, and tendon (Figure 5). The visualization at the whole muscle level and the fiber level are shown in Figures 6 and 7, respectively.

### Activation of Anatomical Muscle Compartments

Wolf and Kim<sup>17</sup> found that the human TA has three distinct neuromuscular compartments (Figure 7). The anterior aspect of the muscle has one partition (A head, Figure 7). The posterior aspect of the muscle has two partitions (B head and C head, Figure 7). Studies in animal muscles<sup>18</sup> have been performed in non-linear summation of force. In these studies parts of the muscle corresponding to neuromuscular compartments

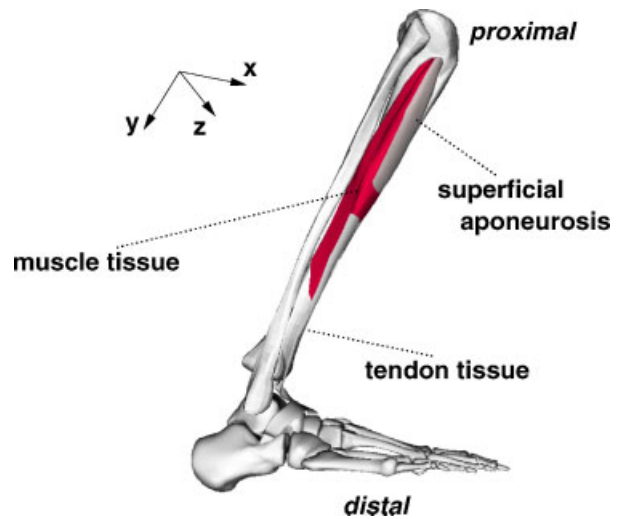


Figure 6. Human TA at the whole muscle level.

are activated separately. Sandercok<sup>18</sup> introduced the non-linear summation of force as

$$F_{nl}(t) = F_{AB}(t) - F_A(t) - F_B(t) \quad (12)$$

where  $F_{AB}(t)$  was described as the force measured when both parts A and B of the muscle are activated together.  $F_A(t)$  and  $F_B(t)$  were described when force of part A and part B, respectively, were stimulated alone.

For the investigation of non-linear summation of muscle force on human TA, a simple theoretical formulation can be adopted. For example,  $F_{AB}(t)$  can be described as the force measured when both the deep and the superficial unipennate half of TA are activated together.  $F_A(t)$  and  $F_B(t)$  can be described when the deep unipennate half of TA and the superficial unipennate half of TA were activated alone.

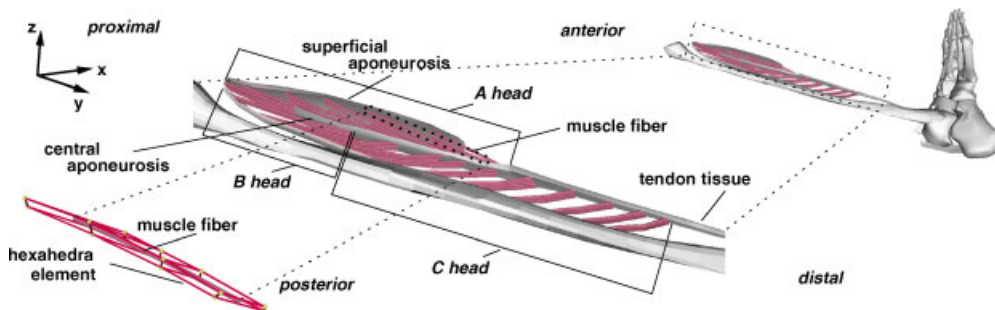


Figure 7. Human TA at the fiber bundle level and muscle compartments.

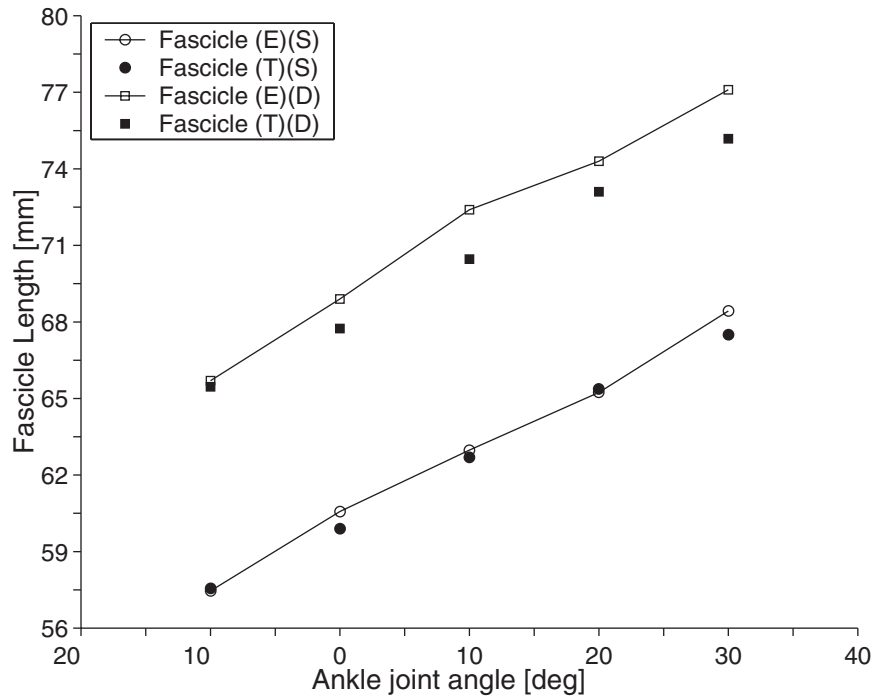


Figure 8. Passive deformations for the experimental (E) and theoretical fascicle lengths (T), for superficial (S) and deep (D) unipennate half.

## Muscle Deformation Simulation and Evaluation

For the simulation, parameters such as boundary conditions and material parameters for the passive structures had to be specified (Figure 5).

In the simulation of the passive deformations, the distal insertion (tendon) is moved passively from the ankle joint of  $-10^{\circ}$  to  $+30^{\circ}$  (Figure 8). Shear modulus ( $\mu$ ) for the superficial aponeurosis, central aponeurosis, and muscle tissue were  $\mu = 15$  MPa,  $\mu = 2$  MPa, and  $\mu = 0.015$  MPa, respectively (Mooney–Rivlin relation). For the tendon, the shear modulus ( $\mu$ ) for the tissue matrix was  $\mu = 10$  MPa (Mooney–Rivlin relation) and the Young's modulus ( $\bar{E}$ ) and parameters  $\alpha$  and  $\bar{w}$  for the tendon (Equation 5) were  $\bar{E} = 2000$  MPa,  $\alpha = 0.015$  (1.5% of  $\bar{E}$ ) and  $\bar{w} = 0.15$  (15.0% of  $\bar{E}$ ), respectively.

In the isometric contraction simulations, the distal insertion (tendon) is moved passively from the ankle joint of  $-10^{\circ}$  to  $+30^{\circ}$ . The muscle is held at the ankle joint of  $+30^{\circ}$  and it is activated to the maximum. In Figure 9, comparisons of fascicle lengths and angle of pennation between simulated and experimental results for different levels of MVC are shown. The

undeformed and deformed geometry at the muscle fiber level at the ankle joint of  $+30^{\circ}$  for maximally and submaximally activated muscle behavior is shown (Figure 10). The simulated muscle force was 270.16 N. When only the deep unipennate half was maximally activated, the force was 175.70 N. And, when only the superficial unipennate half was fully activated, the force was 170.98 N.

For the CPU time statistics, the simulation on a 3.2 GHz Intel Pentium 4 CPU using the full Newton method required approximately 11 hours. Under the same conditions using the Secant method required approximately 5 hours.

## Discussion

It was shown that the continuum muscle model can be used to predict conceptually force production properties and structural changes in human skeletal muscles for maximally and submaximally activated muscle behavior. Regarding the simulation of the internal geometry during deformation, the theoretical predictions for the relaxed fascicle lengths at different ankle joint angles (Figure 8) agreed well with the observed experimental



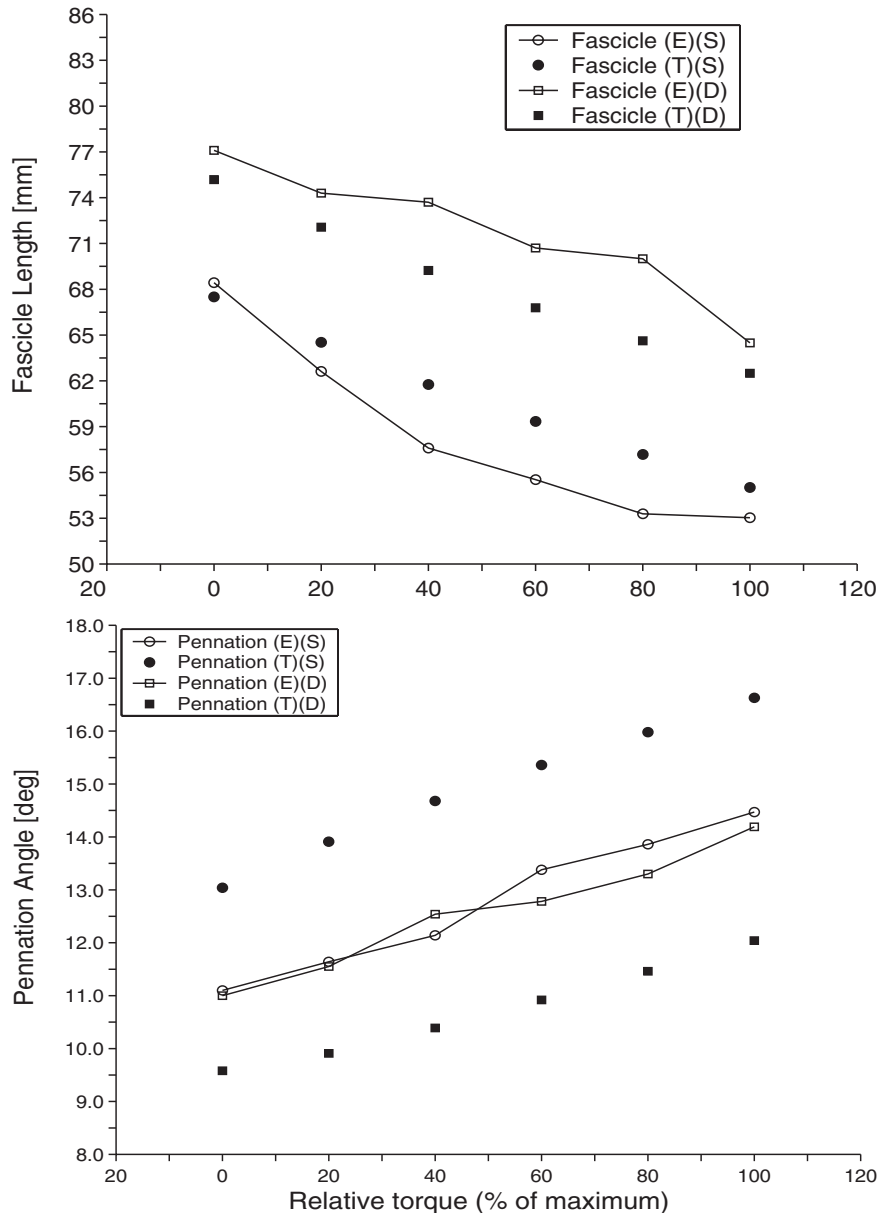


Figure 9. Fascicle lengths and angles of pennation for experimental (E) and theoretical (T) results, for superficial (S) and deep (D) unipennate half.

data. The theoretical predictions for the fascicle lengths and pennation angles at the ankle joint angle of +30° during different levels of maximum activation state show good quantitative and qualitative agreement with the measured experimental data (Figure 9).

Regarding the simulation of the force production properties, the force-length production of the muscle in maximum activation state at ankle joint angle of +30° agreed well with experimental data for maximum vo-

luntary contraction. The following non-linear summation of force was observed during the interaction of the compartments adopted for the human TA:  $(F_{AB}(t) < F_A(t) + F_B(t))$ . The explanation of this observed simulated result is related to the series elasticity of the muscle. This explanation is based on the idea that when more neuromuscular compartments are activated, more muscle fibers will contract. As a result, the increased fibers shortening causes decreasing forces.

The dynamics of muscle contraction is obtained at different structural levels for maximally and submaximally activated muscle behavior which allows for meaningful insight into deformation and contractile process of whole muscle contraction (Figure 10).

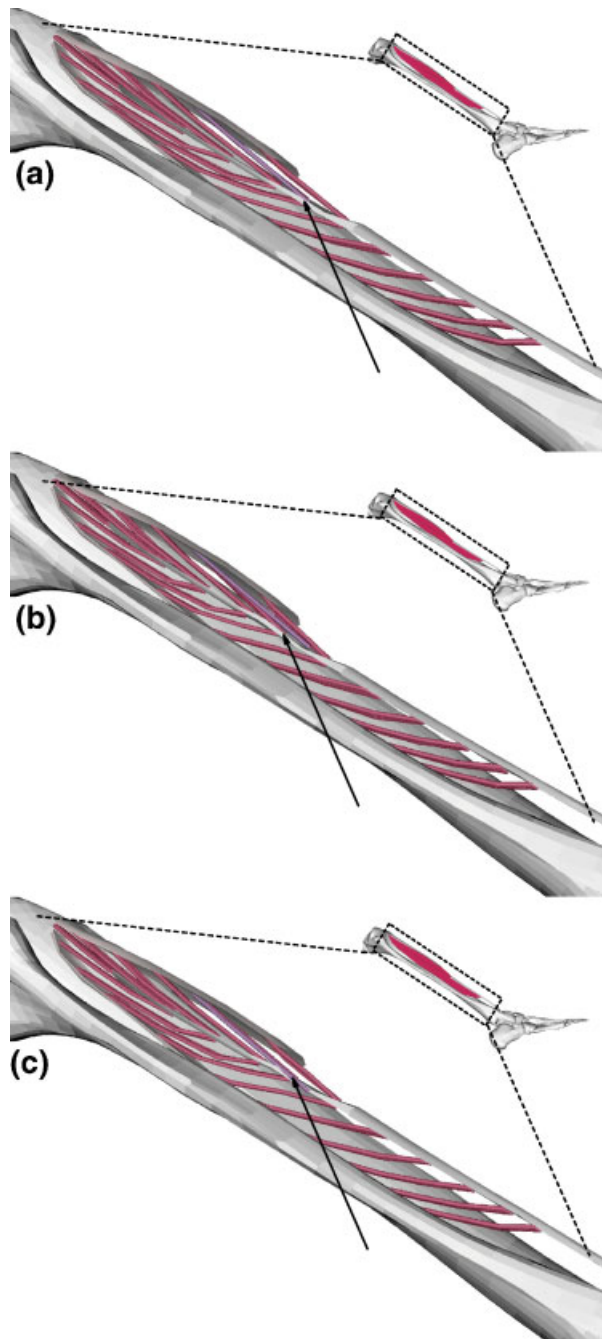


Figure 10. Human TA deformation (a) relaxed state (blue fiber always relaxed) (b) 100% of activation for whole muscle (c) 100% of activation only for the superficial unipennate half.

## Conclusions and Future Work

The proposed model represents a step toward the use of physiologically-based muscle representations in rendering and animation frameworks.

In order to produce the animation of realistic skeletal muscle deformation, and to study muscle function during contraction, models incorporating actual three-dimensional geometries are needed.

Regarding the CPU time statistics, the full Newton's method is more computational expensive than the secant method of Broyden.<sup>19</sup> This is due the fact that the function evaluation is expensive to calculate.

For the modeling and simulation of the human skeletal muscle structure a next step might include the modeling of the three main ankle extensor muscles of the human lower limb (e.g., tibialis anterior muscle, gastrocnemius muscle, and soleus muscle) and the simulation of the human movement during specific tasks (e.g., walking, running, and jumping) exploring the muscle control strategies introduced in this paper for a group of muscles.

## References

1. Marieb E. *Human Anatomy and Physiology*. Benjamin/Cummings: Redwood City, CA, 1995.
2. Maurel W, Wu Y, Magnenat Thalmann N, Thalmann D. *Biomechanical Models for Soft Tissue Simulation*. Springer-Verlag: Berlin, 1998.
3. Hunter P, Robbins P, Noble D. The iups human physiome project. *European Journal of Physiology* 2002; **445**: 1–9. DOI: 10.1007/s00424-002-0890-1.
4. Lemos RR. *Modeling the deformation of skeletal muscle contraction*. Ph.D. dissertation, Dept. of Computer Science, The University of Calgary, Canada, 2004.
5. Lemos RR, Epstein M, Herzog W, Wyvill B. A framework for structured modeling of skeletal muscle. *Computer Methods in Biomechanics and Biomedical Engineering* 2004; **7**(6): 305–317. DOI: 10.1080/10255840412331317398.
6. Scheepers C, Parent R, Carlson W, May S. Anatomy-based modeling of the human musculature. *Computer Graphics*, 1997; pp. 163–172.
7. Wilhems J, Van Gelder A. Anatomically based modeling. *Computer Graphics*, 1997; pp. 173–180.
8. Chen D, Zeltzer D. Pump it up: Computer animation of a biomechanically based model of muscle using the finite element method. *Computer Graphics*, 1992; pp. 89–98.
9. Ng-Thow-Hing V, Fiume E. Application-specific muscle representations. *Proceedings of Graphics Interface'02*, 2002; pp. 107–115.
10. Teran J, Sifakis E, Blemker S, Ng-Thow-Hing V, Lau C, Fedkiw R. Creating and simulating skeletal muscle from the visible human data set. *IEEE Transactions on Visualization and Computer Graphics* 2005; **11**(3): 317–328. DOI:10.1109/TVCG.2005.42.

11. U.S. National Library of Medicine. <http://www.nlm.nih.gov/research/visible/>, date of access (27 April 2005).
12. Maganaris CN, Kawakami Y, Fukunaga T. Changes in aponeurotic dimensions upon muscle shortening: in vivo observations in man. *Journal of Anatomy* 2001; **199**: 449–456. DOI: 10.1046/j.1469-7580.2001.19940449.x.
13. Gielen AWJ, Oomens CWJ, Bovendeerd PHM, Arts T, Janssen JD. A finite element approach for skeletal muscle using a distributed moment model of contraction. *Computer Methods in Biomechanics and Biomedical Engineering* 2000; **3**: 231–244.
14. Oomens CWJ, Maenhout M, van Oijen CH, Drost MR, Baaijens FP. Finite element modelling of contracting skeletal muscle. *Philosophical Transactions of the Royal Society London. Series B.* 2003; **358**: 1453–1460. DOI: 10.1098/rstb.2003.1345.
15. Fernandez JW, Mithraratne P, Thrupp SF, Tawhai MH, Hunter PJ. Anatomically based geometric modelling of the musculo-skeletal system and other organs. *Biomechanics and Modeling in Mechanobiology* 2002; **2**: 139–155. DOI:10.1007/s10237-003-0036-1.
16. Blemker SS, Pinsky PM, Delp SL. A 3d model of muscle reveals the causes of nonuniform strains in the biceps brachii. *Journal of Biomechanics* 2005; **38**(4): 657–665.
17. Wolf SL, Kim JH. Morphological analysis of the human tibialis anterior and medial gastrocnemius muscles. *Acta Anatomica* 1997; **158**: 287–295.
18. Sandercock TG. Nonlinear summation of force in cat soleus muscle results primarily from stretch of the common-elastic elements. *Journal of Applied Physiology* 2000; **89**: 2206–2214.
19. Press W, Flannery B, Teukolsky S, Vetterling W. *Numerical Recipes in C: The art of scientific computing*. Cambridge University Press: Cambridge, 1988.
20. Houbolt JC. A recurrence matrix solution for the dynamic response or elastic aircraft. *Journal of the Aeronautical Sciences* 1950; **17**: 540–550.
21. Herzog W, Leonard T. Force enhancement following stretching of skeletal muscle: a new mechanism. *The Journal of Experimental Biology* 2002; **205**: 1275–1283.
22. Epstein M, Herzog W. *Theoretical models of skeletal muscle*. John Wiley & Sons: Chichester, England, 1998.
23. Ito M, Kawakami Y, Ichinose Y, Fukashiro S, Fukunaga T. Nonisometric behavior of fascicles during isometric contractions of a human muscle. *Journal of Applied Physiology* 1998; **85**: 1230–1235.

**Authors' biographies:**



**Robson R. Lemos** is an adjunct professor in the Department of Computer Science at Universidade de Caxias do

Sul (UCS) in the south of Brazil. He received his Ph.D. in Computer Science from the University of Calgary, Canada. He also holds a M.Sc. degree from the Universidade Federal do Rio Grande do Sul (Brazil) and a B.Sc. degree from the Universidade Federal de Santa Catarina (Brazil), both in Computer Science. His research interests involve computer graphics, continuum mechanics, muscle anatomy and physiology, and virtual medical applications. He is particularly interested in the development and application of physically-based simulation techniques, including the investigation of practical strategies for Biomedical Engineering and Biomechanics problems associated with soft tissue deformation and simulation of biological structures.



**Jon Rokne** is a professor and the former head of the Computer Science Department at the University of Calgary, Canada, where he has been a faculty member since 1970. His research has spanned the areas of interval analysis, global optimization, and computer graphics and he has co-authored four books, several translations, and a number of research papers. He has presented courses and papers at many conferences including Eurographics, Pacific Graphics, and Computer Graphics International. Currently he is the chair of TOC of the IEEE-CS. He has been a visiting professor at the University of Canterbury, New Zealand (1978), University of Freiburg, Germany (1980), University of Grenoble, France (1983, 1984), and University of Karlsruhe, Germany (1984). He holds a Ph.D. in mathematics from the University of Calgary (1969).



**Gladimir V. G. Baranoski** received a Ph.D. in Computer Science from the University of Calgary in 1998. Currently, he is a faculty member at the School of Computer Science and the leader of the Natural Phenomena Simulation Group at the University of Waterloo. The results of his research on biophysically-based rendering have been made available to the graphics community through the publication of articles in journals and conference proceedings. He has also organized

tutorial presentations for conferences (CGI 2000, EUROGRAPHICS (2001 and 2002) and SIGGRAPH (2002 and 2003)), and he has recently authored a book on topics related to his research.



**Yasuo Kawakami** completed Bachelor of Physical Education and Master of Science (Exercise Physiology) degrees at the University of Tokyo between 1983 and 1990, and was given Ph.D. from the University of Tokyo in 1995. Now he is a professor at Faculty of Sport Sciences of Waseda University, lecturing in Biomechanics and Biodynamics. His main research interest is in the area of muscle mechanics, particularly on muscle behavior *in vivo* and during human movements. Effects of training, growth, aging, and fatigue on human muscles are also in the scope of his research. He is a member of Board of Directors of Japanese Society of Biomechanics.



**Toshiyuki Kurihara** is a graduated student in Doctoral Program at Department of Life Sciences (Sports Sciences), University of Tokyo. He received his M.Sc. degree and a B.Sc. degree from the University of Tokyo, Japan. His research interests involve muscle anatomy and physiology, and skeletal muscle modeling.